

# Electrochemical Synthesis of Polyaniline/Montmorillonite Nanocomposites and Their Characterization

Hung Van Hoang and Rudolf Holze\*

*Institut für Chemie, AG Elektrochemie, Technische Universität Chemnitz, 09107 Chemnitz, Germany*

*Received December 7, 2005. Revised Manuscript Received February 13, 2006*

A novel approach to the synthesis of polyaniline–montmorillonite (PANI–MMT) nanocomposites by in situ electropolymerization of anilinium–montmorillonite in 0.3 M sulfuric acid on a gold substrate is reported. The nanocomposites were characterized by elemental analysis, cyclic voltammetry, X-ray diffraction, in situ UV–vis spectroscopy, Fourier transform infrared spectroscopy, and in situ conductivity measurements. Cyclic voltammograms of PANI–MMT are similar to those of PANI synthesized electrochemically under similar conditions. Formation of PANI inside the MMT was confirmed by X-ray diffraction analysis where the  $d$  spacing is increased from 10.09 Å (Na<sup>+</sup>–montmorillonite) to 12.62 Å (PANI–MMT). The C–N stretching vibration ( $\nu_{\text{C–N}}$ ) which appears with PANI at 1296 cm<sup>-1</sup> has been shifted to 1311 cm<sup>-1</sup> for PANI–MMT, indicating the existence of interactions between intercalated PANI and MMT layers. Conductivities of the nanocomposites are almost an order of magnitude lower than those of PANI.

## Introduction

Polyaniline (PANI) is unique in the family of conjugated polymers;<sup>1</sup> it is the most intensively investigated electronically conductive polymer because of its potential commercial applications in, for example, rechargeable batteries, electrochromic display devices, electrochemical sensors, and electrochemical capacitors, and also in active corrosion protection.<sup>2–7</sup> Recently, conducting polymer layered inorganic solid nanocomposites have been the subject of considerable research interest because, being derived from a unique combination of inorganic and organic components, they have possible technological application and raise challenging scientific issues.<sup>8–10</sup> A prominent class of these nanocomposites are materials containing PANI and montmorillonite (MMT; clay minerals), because MMT minerals have attractive properties such as large surface area, ion exchange, and expandability properties. MMT belongs to the general family of 2:1 phyllosilicates composed of stacked layers of aluminum octahedron and silicon tetrahedrons. Substitution of aluminum for magnesium will create an overall negative charge, and this negative charge is compensated by exchangeable metal cations such as Na<sup>+</sup>, K<sup>+</sup>, Ca<sup>2+</sup>, and Mg<sup>2+</sup>.<sup>11,12</sup>

A PANI–MMT nanocomposite can be synthesized either by chemical oxidation of aniline inside the layers or via an electrochemical method. Recently, several reports have been published on chemical methods of synthesis of PANI–MMT nanocomposites<sup>4,6,11,13–17</sup> and some other conjugated polymer–MMT nanocomposites such as poly(pyrrole)–MMT,<sup>18</sup> poly(*o*-methoxyaniline)–MMT,<sup>19</sup> poly(2-ethynylpyridine)–MMT,<sup>20</sup> and poly(thiophene)–MMT.<sup>21</sup>

Electrochemical polymerization of monomers on an electrode surface offers many advantages over chemical methods. The resulting product is a solid, does not need to be extracted from the initial monomer/oxidant/solvent mixture, and is easily amenable to numerous techniques of characterization such as UV–visible, infrared, and Raman spectroscopies and in situ conductometry.<sup>22</sup> Inoue and Yoneyama<sup>23</sup> have reported the electrochemical synthesis of PANI–MMT using a clay modified electrode. Aniline was intercalated by dipping the electrode in aniline followed by drying in air. The electropolymerization was carried out galvanostatically at 20  $\mu\text{A cm}^{-2}$

\* To whom correspondence should be addressed. E-mail: rudolf.holze@chemie.tu-chemnitz.de.

- (1) Huang, J.; Kaner, R. B. *J. Am. Chem. Soc.* **2004**, *126*, 851.
- (2) Gasparac, R.; Martin, C. R. *J. Electrochem. Soc.* **2001**, *148*, B138.
- (3) do Nascimento, G. M.; Constantino, V. R. L.; Landers, R.; Temperini, M. L. A. *Macromolecules* **2004**, *37*, 9373.
- (4) Kim, B. H.; Jung, J. H.; Hong, S. H.; Joo, J. *Macromolecules* **2002**, *35*, 1419.
- (5) Chen, K. H.; Yang, S. M. *Synth. Met.* **2003**, *135–136*, 151.
- (6) Kim, B. H.; Jung, J. H.; Kim, J. W.; Choi, J. H.; Joo, J. *Synth. Met.* **2001**, *117*, 115.
- (7) Conroy, K. G.; Breslin, C. B. *Electrochim. Acta* **2003**, *48*, 721.
- (8) Yoshimoto, S.; Ohashi, F.; Ohnishi, Y.; Nonami, T. *Synth. Met.* **2004**, *145*, 265.
- (9) Tyan, H. L.; Liu, Y. C.; Wei, K. H. *Chem. Mater.* **1999**, *11*, 1942.
- (10) Yeh, J. M.; Chen, C. L.; Chen, Y. C.; Ma, C. Y.; Lee, K. R.; Wei, Y.; Li, S. *Polymer* **2002**, *43*, 2729.

- (11) Zeng, Q. H.; Wang, D. Z.; Yu, A. B.; Lu, G. Q. *Nanotechnology* **2002**, *13*, 549.
- (12) Feng, B.; Su, Y.; Song, J.; Kong, K. *J. Mater. Sci. Lett.* **2001**, *20*, 293.
- (13) Lee, D.; Char, K.; Lee, S. W.; Park, Y. W. *J. Mater. Chem.* **2003**, *13*, 2942.
- (14) Wu, Q.; Xue, Z.; Qi, Z.; Wang, F. *Polymer* **2000**, *41*, 2029.
- (15) Lee, D.; Lee, S. H.; Char, K.; Kim, J. *Macromol. Rapid Commun.* **2000**, *21*, 1136.
- (16) de Azevedo, W. M.; Schwartz, M. O. E.; do Nascimento, G. C.; da Silva, E. F. *Phys. Status Solidi C* **2004**, *1*, S249.
- (17) Kim, J. W.; Kim, S. G.; Choi, H. J.; Jhon, M. S. *Macromol. Rapid Commun.* **1999**, *20*, 450.
- (18) Kim, J. W.; Liu, F.; Choi, H. J.; Hong, S. H.; Joo, J. *Polymer* **2003**, *44*, 289.
- (19) Yeh, J. M.; Chin, C. P. *J. Appl. Polym. Sci.* **2003**, *88*, 1072.
- (20) Liu, H.; Kim, D. W.; Blumstein, A.; Kumar, J.; Tripathy, S. K. *Chem. Mater.* **2001**, *13*, 2756.
- (21) Ballav, N.; Biswas, M. *Synth. Met.* **2004**, *142*, 309.
- (22) Genies, E. M.; Boyle, A.; Lapkowski, M.; Tsintavis, C. *Synth. Met.* **1990**, *36*, 139.
- (23) Inoue H.; Yoneyama, H. *J. Electroanal. Chem.* **1987**, *233*, 291.

in 2 M hydrochloric acid. However, this method does not yield a homogeneous composite because the intercalation is not homogeneous and the excess of aniline is not removed. Feng et al.<sup>12</sup> have also electropolymerized anilinium in MMT potentiostatically at  $E_{\text{SCE}} = 0.8$  V in a pretreated mixture of aniline–MMT and HCl where the final concentration of HCl is 1 M under magnetic stirring. However, the PANI–MMT composite is obtained in the dispersion and not on the surface of the electrode. In a different approach, Chen and Yang have prepared composites by electro-oxidizing MMT loaded with anilinium deposited on a platinum sheet electrode in the presence of further anilinium in the acidic electrolyte solution.<sup>5</sup> The obtained product contained most likely considerable amounts of PANI on the outside of the composite. To our knowledge, so far there has been no report on the electrochemical synthesis of a PANI–MMT nanocomposite by potentiostatic electrolysis of anilinium–MMT dispersions with simultaneous deposition of the nanocomposite on the electrode surface in the form of an adhering film. In this paper, we report a potentiostatic electropolymerization of anilinium–MMT with the simultaneous deposition of nanocomposites on an electrode surface and the characterization of the resulting organic–inorganic hybrid material using cyclic voltammetry, X-ray diffraction (XRD), infrared spectroscopy, in situ UV–vis spectroscopy, and in situ conductivity measurements.

### Experimental Section

Aniline (Merck) was distilled under reduced pressure and stored under nitrogen prior to use. The clay mineral bentonite (ABCR GmbH, Germany) was cation exchanged with a saturated sodium chloride solution, washed with an excess of water, filtered, and dried in an oven at 50 °C for 8 h to get sodium montmorillonite ( $\text{Na}^+$ –MMT). Water (18 M $\Omega$ ; Serapur pro 90C) was used, and all other chemicals were analytical grade reagents and used as received. All solutions were purged with nitrogen before electrochemical measurements.

Anilinium–MMT required for electropolymerization was prepared in the following way. A total of 1 g of  $\text{Na}^+$ –MMT was dispersed in 50 mL of 0.5 M sulfuric acid containing 0.1 M aniline, purged with nitrogen for a few minutes, and stirred for 24 h at room temperature. At pH 1–2 and room temperature, the rate of dissolution of clay is very small ( $10^{-10}$  mol  $\text{m}^{-2}$   $\text{s}^{-1}$ ).<sup>24,25</sup> The dissolution rate increases with increasing temperature and decreasing pH. However, in the intercalation method we have used and within the given time frame, the rate of dissolution has no significant effect on the stability of the anilinium–MMT solution.

The dispersion was filtered and washed with excess of deionized water to remove free anilinium ions. During intercalation, anilinium ions can also be absorbed on the surface of the MMT tactoid as it is structurally the same as the interlayer-oxygen basal plane with exchangeable cations. However, any such absorbed ions were most likely removed during elution with an excess of deionized water. No attempt was made to determine the amount of anilinium in MMT, nor could the fraction of exchanged sodium ions be determined. The resulting wet solid (anilinium–MMT) was dispersed in 20 mL of deionized water and diluted to 50 mL using 0.5 M sulfuric acid with a final concentration of the electrolyte of

0.3 M. Electrochemical polymerization was carried out on a gold sheet electrode at a constant electrode potential of  $E_{\text{SCE}} = 700$  mV at room temperature. Another gold sheet electrode and a saturated calomel electrode (SCE) were used as counter and reference electrodes, respectively. The electrolyte near the working electrode area was kept under slow magnetic stirring (rpm = 80) to maintain the homogeneity of the dispersion. PANI–MMT deposited on the working electrode was washed with deionized water and dried at room temperature. No attempt was made to determine layer thickness. For in situ UV–vis spectroscopy, an indium doped tin oxide (ITO coated glass sheets of surface resistance 20  $\Omega$   $\text{cm}^{-2}$  (MERCK)) coated glass sheet was used as the working electrode, and a constant potential of  $E_{\text{SCE}} = 800$  mV was applied.

**Characterization.** Elemental analysis was carried out using an elemental analyzer Vario EL Elementar Analysensysteme GmbH (Hanau). A custom built potentiostat connected to a computer with an AD/DA converter was used to record cyclic voltammograms (CVs). Electrochemical measurements were carried out in a three-electrode cell under a nitrogen atmosphere. For conductivity measurements<sup>26</sup> a double band gold electrode, a gold sheet counter electrode, and a SCE were used as working, counter, and reference electrodes, respectively. UV–vis spectra were recorded using a Shimadzu UV-2101PC UV–vis spectrophotometer. PANI–MMT deposited on a clean ITO glass was used as the working electrode. A quartz cell of 1 cm path length fitted with a platinum wire as the counter electrode and SCE connected via a salt bridge as a reference electrode served as a three-electrode cell. XRD patterns were obtained on a Seifert FPM/XRD7 diffractometer with Ni-filtered Cu K $\alpha$  radiation ( $\lambda = 0.154$  nm) operated at 40 kV and 30 mA. Infrared spectra were recorded on a BioRad FTS-40 Fourier transform infrared (FT-IR) spectrometer with a liquid-nitrogen-cooled mercury cadmium telluride detector using the KBr pellet technique.

### Results and Discussion

Chemical polymerization of anilinium–MMT takes place easily when a moderately strong oxidizing agent such as ammonium persulfate is used.<sup>15</sup> For comparison we have also polymerized an anilinium–MMT dispersion using 0.1 M ammonium persulfate in a solution without free aniline. Chemical oxidation commenced within 5 min, and the color of the dispersion changed from ash to blue-green. In case of the electrochemical polymerization the color change could be seen only after 30 min and a thick film is obtained after 2.5 h. The electrochemically inactive clay particles hinder the formation of a film on the electrode surface. Formation of a good adherent film on the electrode surface depends on several parameters such as method of synthesis, magnetic stirring, electrolyte used, and concentration of anilinium ions in the clay. Efforts to synthesize PANI–MMT nanocomposites potentiodynamically by cycling in the potential range of  $E_{\text{SCE}} = -200$  to 900 mV failed. PANI–MMT formed this way does not adhere to the electrode when the solution is stirred at higher speed. Therefore, we have used very slow stirring with 80 rotations per minute, which is good enough to maintain the homogeneity of the dispersion. We have also noticed that with HCl as the electrolyte there was no electropolymerization of anilinium–MMT. This may be due to the strong adsorption of  $\text{Cl}^-$  ions on the surface of the

(24) Rufe, E.; Hochella, M. F., Jr. *Science* **1999**, 285, 874.

(25) Amram, K.; Ganor, J. *Geochim. Cosmochim. Acta* **2005**, 69, 2535.

(26) Holze, R.; Lippe, J. *Synth. Met.* **1990**, 38, 99. Lippe, J.; Holze, R. *Synth. Met.* **1991**, 41–43, 2927.

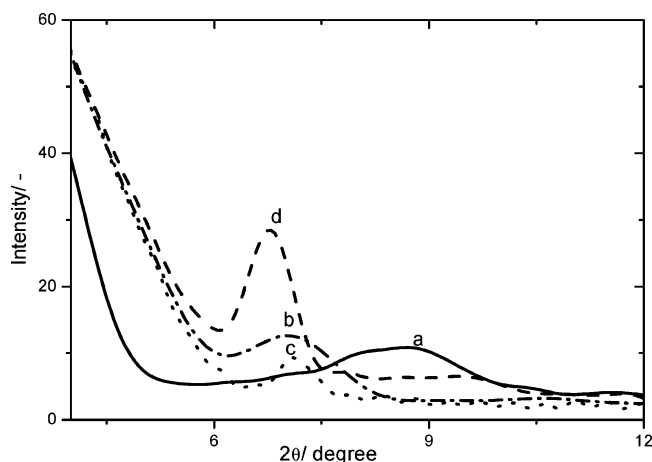


**Figure 1.** XRD patterns of  $\text{Na}^+$ -MMT (a), the oxidized form and (b) and reduced form (c) of PANI-MMT, and anilinium-MMT (d).

gold electrode. PANI-MMT was successfully synthesized using other acids such as  $\text{H}_2\text{SO}_4$ ,  $\text{HClO}_4$ , and oxalic acid. Electropolymerization does not take place when we use lower concentrations of aniline ( $<0.1$  M) whereas higher concentrations of aniline yield free anilinium ions which were removed during washing.

**Elemental Analysis.** Elemental analysis was carried out to calculate the percentage composition of PANI in the nanocomposite; the value is nearly 10 wt %. On the basis of the reported cation exchange capacities of MMT,<sup>27</sup> loadings of 6 wt % of anilinium cations when taking the lower capacity limit and of 13.7 wt % when taking the upper capacity limit were estimated. The observed actual polymer content is well within this range. PANI content in PANI-MMT nanocomposites described elsewhere generally varies in the range from 2 to 12.3 wt %.<sup>3,13-15</sup> Higher contents of PANI have been reported (up to 74.7 wt %), but on the basis of experimental evidence, PANI is deposited on the outside of MMT and not only intercalated.<sup>15</sup> Such deposits may be the result of surface absorption of anilinium ions on the clay. In the procedure employed here based on the polymer content, formation of PANI on the outside of the nanocomposite is highly unlikely because of the strong interaction between the intercalated anilinium cations and the MMT layers which make egress of the anilinium cations very unlikely, whereas the rigorous purge of the aniline-loaded MMT obviously removed any aniline adsorbed on the outer surface; the comparison between possible anilinium loadings and the actually observed polymer content support this conclusion.

**X-ray Diffraction.** Figure 1 shows XRD patterns of the  $\text{Na}^+$ -MMT, anilinium-MMT, PANI-MMT oxidized form, and PANI-MMT reduced form (reduced form of PANI-MMT was obtained by applying a constant potential of  $E_{\text{SCE}} = -200$  mV on a freshly synthesized oxidized sample of PANI-MMT for 10 min). The  $d$  spacing of the material was calculated from the angular position  $2\theta$  of the observed reflection peaks based on the Bragg equation  $\lambda = 2d \sin \theta$ , where  $\lambda$  is the wavelength of the X-rays and  $\theta$  is the scattering angle. As shown in Figure 1, the reflection peak

of the  $\text{Na}^+$ -MMT sample at  $2\theta = 8.8^\circ$  is shifted toward lower angles for anilinium-MMT and PANI-MMT nanocomposites (both oxidized and reduced forms). The  $d$  spacings of the materials are 12.8, 12.6, and 12.5 Å for anilinium-MMT, the PANI-MMT oxidized form, and the PANI-MMT reduced form, respectively. The average  $d$  spacing of the nanocomposites was found to be 12.55 nm. Upon insertion of PANI, the  $d$  spacing is increased from 10 to 12.55 Å, that is, increased by 2.55 Å, which is comparable with reported values (1.3–6.0 Å).<sup>3,8,12-17,28</sup> The diffraction peak of  $\text{Na}^+$ -MMT in Figure 1 is broader than with PANI-MMT whereas the peak of anilinium-MMT is intense and sharp. The sharpness of the peaks can be influenced by crystallinity or clay-layer stacking order. Thus, the broader peak of  $\text{Na}^+$ -MMT indicates less crystallinity and order of clay-layer stacking than the other samples.<sup>14,29,30</sup>

**Cyclic Voltammetry.** CVs of PANI-MMT nanocomposites, deposited on a gold electrode, were recorded in an aqueous solution of 0.5 M  $\text{H}_2\text{SO}_4$  with different thicknesses as obtained after different times of electropolymerization of the PANI-MMT films (Figure 2). CVs of PANI exhibit two pairs of redox waves with the first one observed at  $E_{\text{SCE}} = 200$  mV indicating the transformation of the leucoemeraldine form into the conducting emeraldine form and the second one at  $E_{\text{SCE}} = 810$  mV which is due to the conversion of the emeraldine into the pernigraniline form. A pair of humps in the region of  $E_{\text{SCE}} = 0.30$ – $0.50$  V has been assigned to overoxidation products.<sup>31,32</sup> The shape of the CVs of PANI-MMT is similar to those of PANI. This indicates that clay layers do not influence the electrochemical properties of PANI nor does the intercalation favor a polymer with different properties (such as, e.g., molecular weight) as far as could be evidenced with this electrochemical technique. There is only a minor shift of the reduction peak associated with the pernigraniline-emeraldine transition which might indicate some not yet understood interaction between PANI and MMT. It was also observed that the PANI-MMT film was stable as it was not damaged/peeled off from the surface of the electrode even with continuous potential cycling for up to 20 cycles (Figure 2c); changes in the CVs implying degrading or loss of active material are minor only. The electrochemical activity of the nanocomposite was also checked in a neutral unbuffered aqueous solution of 0.5 M KCl by recording CVs in the range of  $-0.20$  to  $+0.85$  V (Figure 2d). The figure demonstrates that electroactivity of the nanocomposite is retained even at neutral pH. However, the single redox wave observed cannot be attributed to a specific redox process currently.

**FT-IR Analysis.** Figure 3 shows FT-IR spectra of  $\text{Na}^+$ -MMT, pure PANI, the mechanical mixture of PANI/ $\text{Na}^+$ -MMT (i.e., an unintercalated system), and electrochemically deposited PANI-MMT. The characteristic vibrations of

(27) Meier, L. P.; Nüesch, R. *J. Colloid Interface Sci.* **1999**, *217*, 77.

(28) Yoshimoto, S.; Ohashi, F.; Kameyama, T. *Macromol. Rapid Commun.* **2004**, *25*, 1687.

(29) Ma, Z.; Kyotani, T.; Tomita, A. *Chem. Commun.* **2000**, 2365.

(30) Welch, M. D.; Keppe, A. K.; Jephcoat, A. P. *Am. Mineral.* **2004**, *89*, 1337.

(31) Abd-Elwahed, A.; Holze, R. *Synth. Met.* **2002**, *131*, 61.

(32) Holze, R. In *Handbook of Advanced Electronic and Photonic Materials*; Nalwa, H. S., Ed.; Gordon and Breach & OPA N.V.: Singapore, 2001; Vol. 2, p 171.

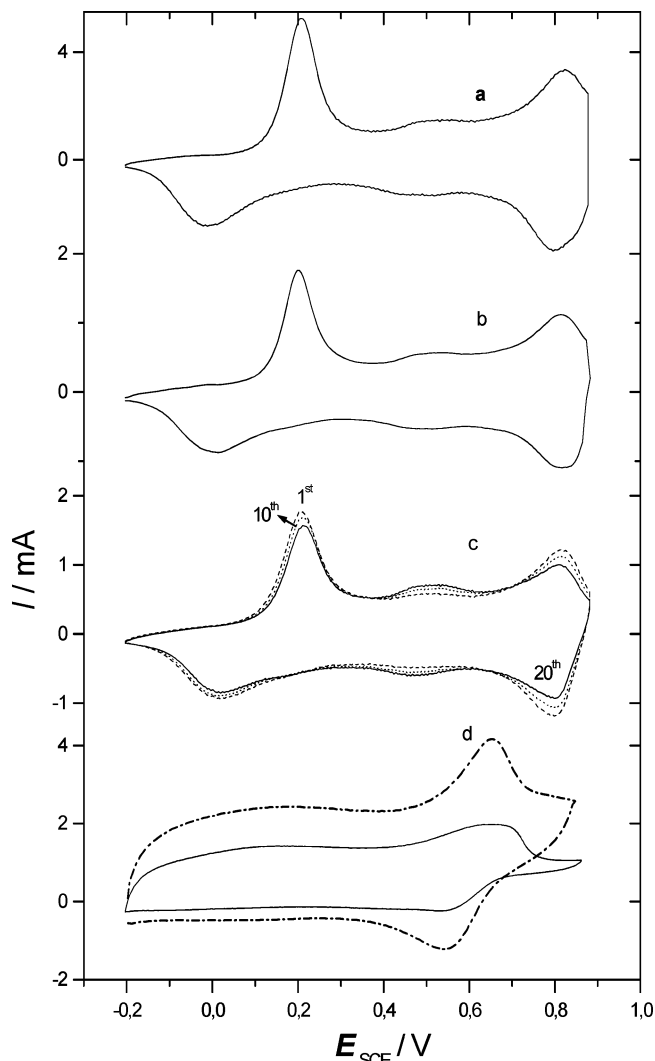


**Figure 2.** CV of (a) PANI, (b) PANI-MMT, and (c) PANI-MMT (1st, 10th, and 20th cycles) recorded in 0.5 M H<sub>2</sub>SO<sub>4</sub>. (d) PANI (dashed line) and PANI-MMT (solid line) recorded in 0.5 M KCl at a scan rate of 100 mV/s.

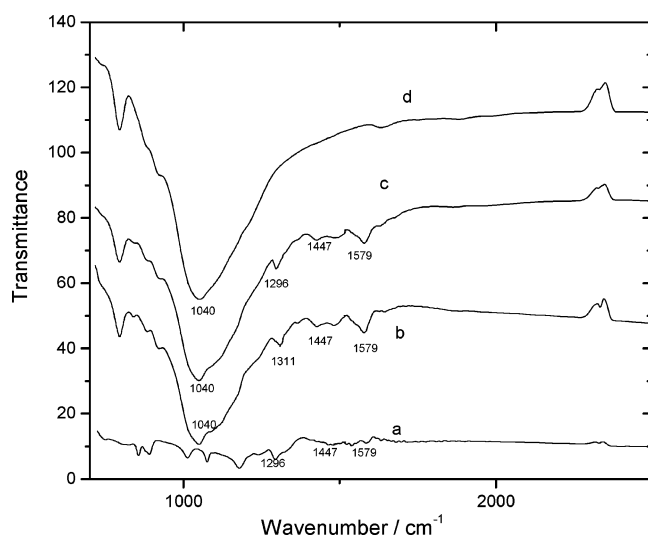


**Figure 3.** FT-IR spectra of PANI (a), electrochemically synthesized PANI-MMT (b), mechanical mixture of PANI and MMT (c), and Na<sup>+</sup>-MMT (d).

Na<sup>+</sup>-MMT and the emeraldine salt are known to be in the region between 700 and 1700 cm<sup>-1</sup>.<sup>13</sup> The major bands

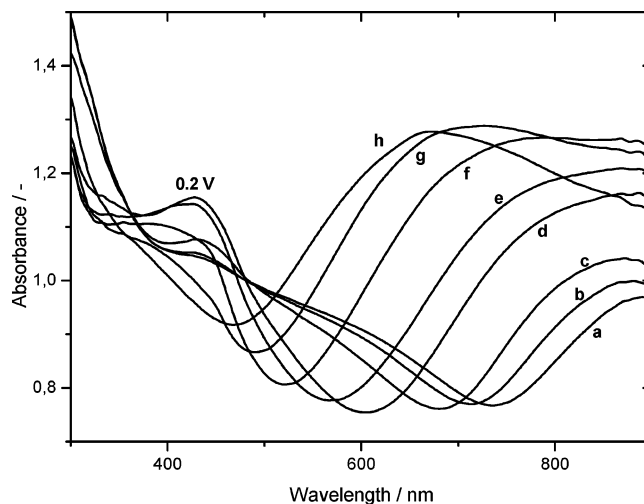


**Figure 4.** In situ UV-vis spectra of PANI-MMT recorded in 0.5 M H<sub>2</sub>SO<sub>4</sub> at different positive potentials (V): -0.20 (a), 0.0 (b), 0.10 (c), 0.20 (d), 0.30 (e), 0.50 (f), 0.70 (g), and 0.80 (h).

associated with Na<sup>+</sup>-MMT appear at 1040 cm<sup>-1</sup> ( $\nu_{\text{Si-O}}$ ) and 918 cm<sup>-1</sup> ( $\delta_{\text{Al-OH}}$ ).<sup>14,16</sup> The characteristic absorption bands of PANI appear at 1296 ( $\nu_{\text{C-N}}$ ), 1477, and 1579 cm<sup>-1</sup> ( $\nu_{\text{C=C}}$  of benzenoid and quinoid rings, respectively).<sup>33</sup> FT-IR spectra of PANI-MMT composites exhibit bands characteristic of PANI as well as of MMT, which confirms the presence of both components in the PANI-MMT composite. FT-IR spectra of the mechanical mixture of PANI and MMT are slightly different from the spectra of electrochemically synthesized PANI-MMT. The band at 1296 cm<sup>-1</sup> in the spectrum of a mechanical mixture of PANI and MMT is shifted to 1311 cm<sup>-1</sup> in the spectra of the intercalated nanocomposites (Figure 3). This shift is due to the physicochemical interaction (hydrogen bonding between the -NH group of PANI and -O of silicate) in the intercalated PANI-MMT<sup>13,15</sup> whereas mechanical mixtures of PANI and MMT lack such an interaction. A similar trend was observed by Stutzmann and Siffert for the acetamide-MMT system. They found the C-N stretching vibration of acetamide observed at 1380 cm<sup>-1</sup> shifted to higher wavenumbers (1400 cm<sup>-1</sup>) after adsorption onto a clay surface; they have attributed this shift to the hydrogen bonding between NH<sub>2</sub> groups of acetamide and oxygen atoms of the basal surface of the clay.<sup>34</sup>

**In Situ UV-Vis Spectroscopy.** For in situ UV-vis measurements, the PANI-MMT nanocomposite was deposited on the ITO glass electrode at a constant potential of  $E_{\text{SCE}} = 800$  mV. Figure 4 shows in situ UV-vis spectra of PANI-MMT on an ITO electrode at various electrode potentials recorded in the 0.5 M H<sub>2</sub>SO<sub>4</sub>. PANI exhibits three electronic absorption bands at 320, 430, and ~800 nm which are assigned to a  $\pi \rightarrow \pi^*$  transition, radical cations, and polarons, respectively.<sup>35-37</sup> Electronic absorption spectra of PANI-MMT like PANI exhibit bands at 430 and 870 nm, but the band at 320 nm could not be seen. Absorbance of

(33) Harada, I.; Furukawa, Y.; Ueda, F. *Synth. Met.* **1989**, *29*, E303.

(34) Stutzmann, Th.; Siffert, B. *Clays Clay Miner.* **1977**, *25*, 392.

(35) Hochfeld, A.; Kessel, R.; Schultze, J. W.; Thyssen, A. *Ber. Bunsen-Ges. Phys. Chem.* **1988**, *92*, 1406.

(36) Stilwell, D. E.; Park, S. M. *J. Electrochem. Soc.* **1989**, *136*, 427.

(37) D'Aprano, G.; Leclerc, M.; Zotti, G. *Macromolecules* **1992**, *25*, 2145.

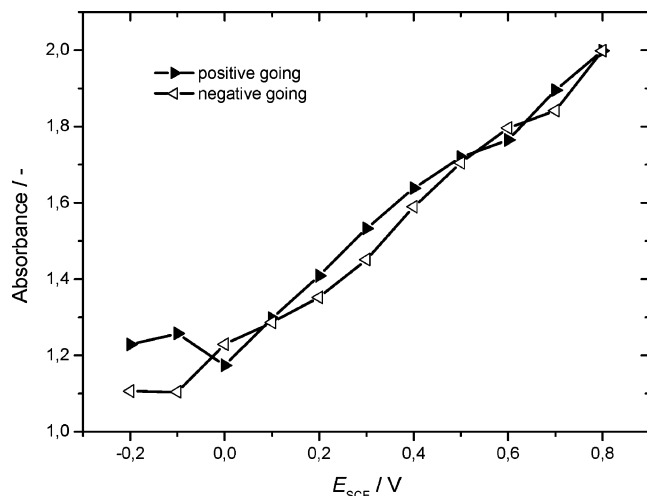


**Figure 5.** Plot of absorbance at 670 nm versus applied electrode potential for PANI–MMT.

the band at 430 nm reaches a maximum at  $E_{SCE} = 0.20$  V which indicates higher concentration of radical cations at this applied potential. At this applied potential ( $E_{SCE} = 0.20$  V) the first oxidation wave in the CV of PANI–MMT which corresponds to the leucoemeraldine-to-emeraldine transition has a maximum peak current (Figure 2). By shifting the electrode potential to higher values, the intensity of this band diminishes. When the applied potential is increased from  $E_{SCE} = -0.20$  to  $E_{SCE} = 0.70$ , maximum positions of the band at 870 nm (polaronic transition) are shifted into the near-infrared (NIR) region, and at  $E_{SCE} = 0.70$  this band becomes more flattened. A similar trend was observed by Malinauskas et al.<sup>38</sup> for potentiostatically ( $E_{RHE} = 1.20$  V) prepared PANI. When the applied potential is increased further to  $E_{SCE} = 0.80$  V, the polaronic band in the NIR region disappears and a new band at 670 nm appears, which is attributed to the blue nonconducting pernigraniline state of PANI. The CV of PANI–MMT has a second oxidation wave at  $E_{SCE} = 0.80$  V corresponding to the emeraldine-to-pernigraniline transition.

In situ electronic absorption spectra of PANI–MMT were also recorded during a stepwise cathodic potential sweep. Figure 5 shows a plot of absorbance at 670 nm versus applied potential recorded with the electrode potential going into the positive and negative directions. Both traces are very close to each other in the potential range of  $E_{SCE} = 0$ – $0.80$  V, indicating a good electrochemical reversibility of the PANI–MMT nanocomposite. Figures 4 and 5 also reveal that electrochromism of PANI in the PANI–MMT nanocomposite is almost retained.

**In Situ Conductivity Measurements.** Resistance values of PANI and PANI–MMT deposited at  $E_{SCE} = 700$  mV were measured in an aqueous solution of 0.5 M  $H_2SO_4$  in the range of  $-0.20 < E_{SCE} < +0.90$  V in the anodic direction and then in the reverse cathodic direction. The  $\log R$  values of

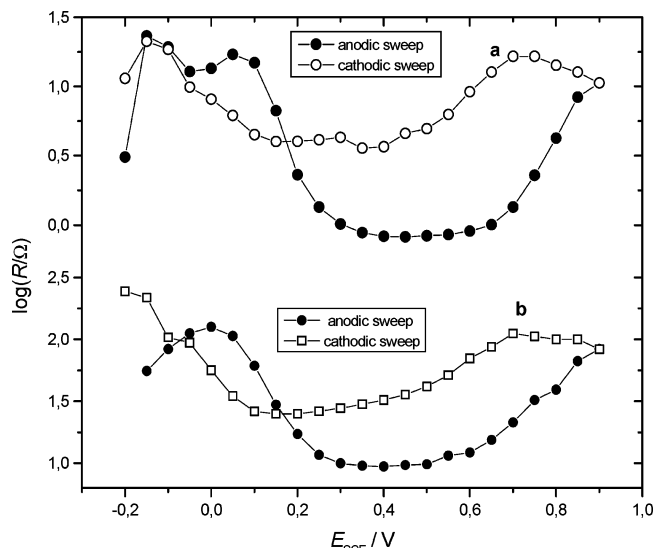


**Figure 6.** Plot of  $\log R$  versus applied electrode potential for PANI (a) and PANI–MMT (b) in an aqueous solution of 0.5 M  $H_2SO_4$ .

both PANI and PANI–MMT against the applied electrode potential are displayed in Figure 6. Two transitions can be observed in the resistivities of both PANI and PANI–MMT. The first transition appears at around  $E_{SCE} = 0$  V where the resistivity values start to decrease, and the second transition appears at around  $E_{SCE} = 0.60$  V where again the resistivity begins to increase. Thus in the potential range of  $E_{SCE} = 0.0$ – $0.60$  V, PANI as well as PANI–MMT is highly conducting; this is the potential range where PANI is in the emeraldine state. When the potential sweep direction was reversed from  $E_{SCE} = 0.90$  to  $-0.20$  V, almost similar trends were observed; however, the conductivities are lower than in the anodic sweep. This loss of in situ conductivity in the reverse cathodic sweep was attributed to partial degradation of PANI at  $E_{SCE} = 0.90$  V.<sup>37</sup> The apparent resistivity of PANI–MMT is higher than that of PANI. In the absence of data enabling the conversion of resistivities into specific resistivities a quantitative comparison is impossible. The slightly smaller relative change of resistivity in case of the nanocomposite may be due to the high fraction (90%) of inert MMT.

## Conclusion

A protocol for the electropolymerization of aniline incorporated into the channels of MMT has been described. PANI–MMT nanocomposite thus formed is adherent to the electrode surface. The conductivities of the composites with 10 wt % of PANI are almost an order of magnitude lower than those of PANI. FT-IR studies reveal the presence of hydrogen bonding between the amine group of PANI and oxygen atoms of clay. Electrochemical properties and in situ UV–vis response of the composites are almost similar to those of PANI.